Available online at www.sciencedirect.com
SCIENCE DIRECT®
Journal of Sound and Vibration 290 (2006) 508–518
JOURNAL OF SOUND AND VIBRATION
www.elsevier.com/locate/jsvi

Short Communication

# On the application of B-spline approximation in structural intensity measurement

C.Q. Wang[a,b,*], E.H. Ong[a], H. Qian[a], N.Q. Guo[b]

[a]*Data Storage Institute, DSI Building, No. 5 Engineering Drive 1, 117608, Singapore*
[b]*School of Mechanical and Production Engineering, Nanyang Technological University, 639798, Singapore*

Received 2 January 2004; received in revised form 15 September 2004; accepted 12 April 2005
Available online 11 July 2005

## 1. Introduction

Evaluation of structural intensity in engineering structures is a field of increasing interest in connection with vibration analysis and noise control. In contrast to classical techniques such as modal analysis, structural intensity indicates the magnitude and direction of the vibratory energy travelling in the structures, which yields information about the positions of the sources/sinks, as well as the energy transmission path. Since structural intensity is directly related to the energy level, proper damping treatments and mechanical modifications can then be adopted to dissipate or divert the structure borne sound efficiently and effectively [1].

Since the first introduction and early developments of structural intensity concept [2–4], many measurement methods and numerical prediction approaches have been proposed. For measurement on plate-like structures (plates, shells and their assemblies, etc.), the determination of structural intensity requires the information of surface velocity and stress, as well as the associated phase relationship between them. The initial works [2–4] on structural intensity measurement are mainly conducted with contact transducers such as accelerometers and strain gauges. Later, to overcome the obvious drawbacks of such method, e.g. additional weight introduced by the sensors, non-contact measurement method is proposed based on near-field acoustic [5]. Currently, optical measurement using laser Doppler vibrometer (LDV) or scanning

*Corresponding author. Tel.: +65 6874 8660; fax: +65 6777 2053.
*E-mail addresses:* cqwang@pmail.ntu.edu.sg, chunqiwang@163.com (C.Q. Wang).

0022-460X/$ - see front matter 
doi:10.1016/j.jsv.2005.04.011

LDV has become a popular technique in the experimental study of structural intensity [6,7,9,10,12,14]. Besides the experimental study, numerical prediction of structural intensity using finite element method (FEM) has also been developed [1,8]. However, because of the difficulty to accurately model the real boundary conditions and dynamic loadings of the structures, the experimental study is preferable to numerical simulation for determination of the structural intensity under various operating conditions.

According to the theoretical formulations for plate-like structures, the structural intensity can be experimentally determined by the measured normal velocity and its spatial derivatives if only the flexural waves are considered. As only the normal velocity or displacement can be obtained through the vibration measurement, finite difference approximation or spatial Fourier transform (SFT) is usually adopted to get the necessary high-order derivatives. The finite difference approximation is first used in Refs. [2,3]. When the contact measurement method is used, finite difference approximation is an appropriate way due to the limited number of measurements. For spatial dense measurements using optical techniques or likes, SFT is usually employed to extract the structural intensity from the velocity measurements [5,9,10,14]. The superiority of SFT over finite difference approximation has been addressed in Refs. [9,10].

The key to calculate the structural intensity through SFT is to obtain a good estimation of the wavenumber spectrum ($k$-space) that results in an accurate representation of the spatial derivatives. Since high-order derivatives are required in the structural intensity formulation, errors in the estimation of wavenumber spectrum, especially at high wavenumber, may be greatly magnified and lead to serious distortion in the calculated structural intensity. Therefore, low-pass $k$-space filter is usually used to remove noise at high wavenumber. The characteristics and performance of the $k$-space filtering have great effects on the accuracy of the structural intensity calculation [9,14].

Geometrical discontinuities (e.g. holes) and non-periodic vibration velocity field (e.g. in a finite plate) often exist in real structures, which may result in large distortions in the estimation of wavenumber spectrum. Irregularly shaped plate and non-equally-spaced measurement points can also pose a challenge to the calculation since rectangular measurement zone and equally spaced data are assumed in the implementation of SFT. Regressive discrete Fourier transform can minimise the errors due to non-periodicity and is also able to deal with non-equally-spaced and non-rectangular-domain data [11]. However, the algorithm is sometimes hard to be automatically used because of trial-and-error parameters [10]. Windowing [14] and mirror processing [10] can be used prior to SFT to minimise the leakage effect due to signal non-periodicity. Although, these methods may partially solve the problems mentioned above with additional operations, useful information may be lost through windowing [14]. Hence, a better data processing scheme may benefit the structural intensity measurement in practice.

B-spline approximation is a common tool for representing and differentiating arbitrary scattered measurement data. If the measured velocity data are approximated with B-splines of degree $n$, then the derivatives up to $(n-1)$ order of the measurement data can be obtained based on the properties of B-spline approximation. Therefore, structural intensity can be calculated from measured velocity data by B-spline approximation. However, like in the case of SFT, issues such as $k$-space filtering must be investigated to guarantee the accuracy and reliability of the obtained results. In Ref. [12], a B-spline approximation-equivalent procedure is introduced to visualise the spatially continuous power flow (structural intensity) in a simply supported plate.

The capability of the proposed method is illustrated through comparing the model convergence of various different meshes.

The present work investigates the performance of B-spline approximation in structural intensity calculation from the viewpoint of $k$-space filtering. Relationship between parameters of B-spline approximation (mesh size) and the $k$-space filter is established, which can help to choose the appropriate mesh size and improve the understanding of the application of B-spline approximation in the structural intensity. In addition, as an advantage of B-spline approximation, the capability of dealing with discontinuities and non-periodicity in signal is also discussed. Finally, vibration measurement is carried out on a thin aluminium plate with arbitrary boundary conditions and the structural intensity distribution calculated is presented and discussed.

## 2. Formulas for structural intensity

The expressions for structural intensity in plate-like structures have been well established in literatures [1–3,10,13,14]. Therefore, only a brief outline is presented here.

Structural intensity is defined as the net energy flow per unit area in the given directions. This definition of structural intensity has the same physical meaning as the acoustical intensity in a fluid medium. The structural intensity in $n$th direction in frequency domain is given by [13]

$$I_n = -\tfrac{1}{2}\mathrm{Re}(\tilde{\sigma}_{nl}\tilde{v}_l^*), \quad n,l = 1,2,3, \tag{1}$$

where $\tilde{\sigma}$ is the complex amplitude of stress, $\tilde{v}_l^*$ is the complex conjugate of the velocity. Here, $\tilde{}$ represents complex quantities and $^*$ indicates complex conjugate.

In plate-like structures, structural intensity can be conveniently defined as the net energy flow per unit length in a given direction. For thin plates, if only the flexural waves are considered, the structural intensity in $x$ and $y$ directions can be written in terms of the normal velocity $v(x,y)$ [10],

$$I_x = \frac{B}{2\omega}\mathrm{Im}\left\{\frac{\partial}{\partial x}(\nabla^2\tilde{v})\tilde{v}^* - \left(\frac{\partial^2\tilde{v}}{\partial x^2} + \upsilon\frac{\partial^2\tilde{v}}{\partial y^2}\right)\frac{\partial\tilde{v}^*}{\partial x} - (1-\upsilon)\frac{\partial^2\tilde{v}}{\partial x\partial y}\frac{\partial\tilde{v}^*}{\partial y}\right\}, \tag{2a}$$

$$I_y = \frac{B}{2\omega}\mathrm{Im}\left\{\frac{\partial}{\partial y}(\nabla^2\tilde{v})\tilde{v}^* - \left(\frac{\partial^2\tilde{v}}{\partial y^2} + \upsilon\frac{\partial^2\tilde{v}}{\partial x^2}\right)\frac{\partial\tilde{v}^*}{\partial y} - (1-\upsilon)\frac{\partial^2\tilde{v}}{\partial x\partial y}\frac{\partial\tilde{v}^*}{\partial x}\right\}, \tag{2b}$$

where $B = Eh^3/12(1-\upsilon^2)$ is the bending stiffness coefficient, $E$ is Young's modulus, $h$ is the plate thickness, $\upsilon$ is the Poisson ratio and $\omega$ the angular frequency.

Therefore, the structural intensity in plates can be determined solely from knowledge of the transverse movements, in the form of products of different space derivatives of the vibration velocity in the normal direction.

## 3. Calculation of structural intensity with B-spline approximation

After the data acquisition in an experiment, a set of discrete velocity data points $(x_r, y_r, \hat{v}_r), r = 1,\ldots,m$, with $(x_r, y_r)$ over the measurement region $R = [a,b]\times[c,d]$, are obtained.

According to Eq. (2), derivatives of normal velocity $v(x, y)$ up to third order must be determined to extract the structural intensity.

B-spline approximation is well suited for estimating multiple-order derivatives. In order to implement the approximation, the region $R$ is subdivided into $(g+1) \times (r+1)$ subrectangles with given knots $\lambda_i$, $i = 0, \ldots, g+1$ ($\lambda_0 = a$, $\lambda_{g+1} = b$), in the $x$ direction and $\mu_j$, $j = 0, \ldots, h+1$ ($\mu_0 = c, \mu_{h+1} = d$), in the $y$ direction. Suppose B-spline of degree $n$ is employed in both $x$ and $y$ direction, and $(\lambda_i, \mu_j)$ are equally spaced over $R$, then the approximation $v(x, y)$ of the measured velocity $\hat{v}_r$ can be expressed as a tensor product spline [15],

$$v(x, y) = \sum\sum \alpha_{i,j} N_i(x) N_j(y),$$

$$i = -\frac{n-1}{2}, \ldots, g + \frac{n+1}{2}, \quad j = -\frac{n-1}{2}, \ldots, h + \frac{n+1}{2}, \tag{3}$$

where $\alpha_{i,j}$ are the coefficients to be determined. $N_i(x)$ and $N_j(y)$ are obtained by scaling and shifting the symmetrical B-spline of degree $n$, $\beta^n(x)$,

$$N_i(x) = \beta^n((x - i)(g + 1)/(b - a)), \tag{4a}$$

$$N_j(y) = \beta^n((y - j)(h + 1)/(d - c)). \tag{4b}$$

The requested coefficients $\alpha_{i,j}$ are determined by minimising the errors between the measured velocity and the approximated one. Here, least-squares criteria is adopted to minimise the squared residual error $\prod$, which is defined as

$$\prod = \sum (v_i - \hat{v}_i)^2. \tag{5}$$

With the coefficients $\alpha_{i,j}$ solved, the velocity at any point $(x_i, y_j) \in R$ can then be computed from Eq. (3). Because the basis function $\beta^n(x)$ leads to splines that is continuous in the $(n-1)$th derivative and smooth derivative in the $(n-2)$th order, $n = 5$ is chosen in this paper. As a result, the reconstructed velocity field is able to offer the third-order smooth derivatives necessary for the structural intensity calculation.

## 4. Performance discussion

Since structural intensity is only a fraction of the total vibratory energy in the structures and high-order derivatives are used in its calculation, it is very sensitive to the noise in the measurement data. The mesh size of the B-spline approximation affects the accuracy of the structural intensity calculated greatly. If a coarse mesh is used, useful information may be lost. However, if the mesh is too fine, too much noise may be kept in the reconstructed velocity field and results in distorted structural intensity map. The relationship between the mesh size and the $k$-space filtering is investigated here. With the relationship established, one can locate the appropriate mesh conveniently and reduce the trial times. After that, the capability of dealing with signal discontinuities and non-periodicity is discussed.

### 4.1. k-space filtering

The purpose of filtering is to remove the noise-contaminated components, especially at high wavenumbers. According to the principle of modal superposition, when a system is excited with a single frequency $f$, all of its eigenmodes are excited but with different degrees of strength. Although the overall response of the structure is a combination of all its natural mode shapes, usually only those modes that make a significant contribution to the motion need to be considered to determine the structural response. Therefore, the filter should be selected as such that it is capable of removing the noise at high wavenumbers (corresponding to high frequencies) while keeping the significant mode shapes at the same time.

When SFT is used, an oval filter is usually employed. It is a low-pass $k$-space filter, and can be described as follows [14]

$$F(k_x, k_y) = \begin{cases} 1 - \dfrac{e^{-\alpha}}{2} & \text{for } r < c \\ \dfrac{e^{-\alpha}}{2} & \text{for } r > c \end{cases} \tag{6}$$

where $\alpha = (1 - r/c)/s$, $r = \sqrt{k_x^2 + k_y^2}$, $c = \sqrt{c_x^2 + c_y^2}$, $c_x^2/a_x^2 + c_y^2/a_y^2 = 1$, and $s$ controls the filter slope. The bandwidth of the low-pass filter can be adjusted in $k_x$ and $k_y$ direction by changing the values of $a_x$ and $a_y$. The determination of the filter parameters, i.e., $a_x$, $a_y$ and $s$ is a trial-and-error process.

The following work demonstrates that the low-pass filtering can also be realised through the least-squares B-spline approximation described in Eq. (3). Generally, least-squares B-spline approximation is used as a data reduction method [17], but it is considered as a noise reduction procedure in this work. In order to illustrate the low-pass filtering effect of B-spline approximation, take a B-spline function $s(x)$ in one dimension for example,

$$s(x) = \sum_{i=-\infty}^{+\infty} c_i \beta^n(x - i). \tag{7}$$

Here, $c_i$ is the B-spline coefficients. Eq. (7) can be seen from another perspective by expressing $s(x)$ in terms of the discrete function values themselves [16]

$$s(x) = \sum_{k=-\infty}^{+\infty} s(k)\eta^n(x - i), \tag{8}$$

where $\eta^n(x)$ is the cardinal spline corresponding to $\beta^n(x)$. Evaluating the function $s(x)$ in Eq. (8) at an integer value $i$, gives,

$$s(i) = \sum_{k=-\infty}^{+\infty} g(k)\eta^n(i - k) \tag{9}$$

which has the exact form of a discrete convolution. The cardinal spline $\eta^n(x)$, evaluated at integer values, is digitally convolved with the sampled values of the function $g(x)$. Therefore, $\eta^n(x)$ works as a digital filter. Aldroubi et al. [16] further proved that the frequency response of the cardinal

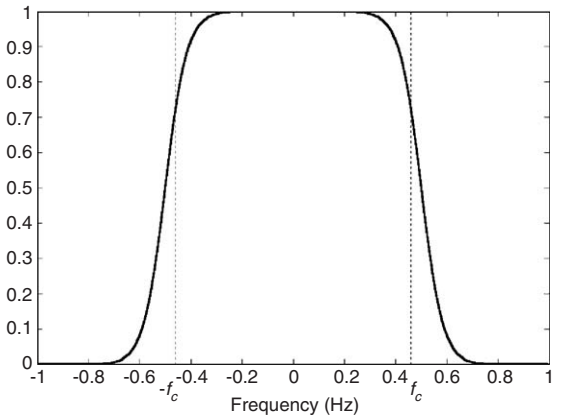


Fig. 1. Fourier transform of the cardinal quintic spline $\eta^5(x)$.

spline converges to the ideal low-pass filter $\mathrm{sinc}(f) = (\sin(\pi f)/\pi f)$ as the order $n$ tends to infinity. Fig. 1 displays the Fourier transform of the quintic cardinal spline $\eta^5(x)$. Apparently, $\eta^5(x)$ works as a low-pass filter and the upper cut-off frequency, $f_c$, is also indicated in Fig. 1.

The results in the one-dimension case are directly applicable to the two-dimensions case through the use of tensor product splines. Thus, after approximation, only components with wavenumbers $k_x$ and $k_y$ satisfying the following conditions are kept in the reconstructed velocity field

$$k_x < 2\pi f_c((h+1)/(b-a)), \tag{10a}$$

$$k_y < 2\pi f_c((g+1)/(d-c)). \tag{10b}$$

Hence, the $k$-space filtering needed to calculate the structural intensity is implemented. Based on Eqs. (10a) and (10b), the bandwidth of the low-pass filter can be easily adjusted by changing the values of $h$ and $g$. The finite element-based procedure in Ref. [12] is equivalent to the approximation process described in this article. If a uniform mesh is adopted with a mesh size $l_x \times l_y$, the band limits of the $k$-space filtering are then $k_x < 2\pi f_c(1/l_x)$ and $k_y < 2\pi f_c(1/l_y)$, respectively.

It is worth noting that, in contrast to the oval filter usually used in SFT, the low-pass filter used here is rectangular. The difference in the shape of the two filters is shown in Fig. 2 by applying the two methods to a white noise field, respectively. Fig. 2(a) illustrates the 2-D $k$-spectrum of the white noise field with an oval low-pass filter. Fig. 2(b) shows the $k$-spectrum of the reconstructed data field with B-spline approximation.

### 4.2. Signal irregularities

One basic property of B-splines is local support [15], which means that the defined segments in Eq. (3) depend just on a few of the coefficients. These coefficients in turn depend on locally measured data. As a result, discontinuities due to holes, irregular scanning shapes, etc., can be

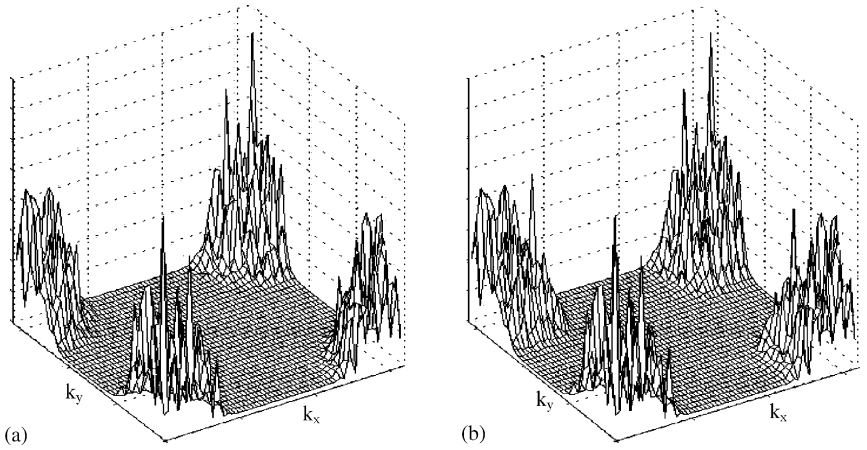


Fig. 2. Fourier transform of a white noise field: (a) with an oval low-pass filter; (b) reconstructed with B-spline approximation.

manipulated with little effect on the overall performance of the reconstructed velocity field. Another important issue is that both the knots in Eq. (3) and the measured points are not necessarily equally spaced, which means the velocity field can be reconstructed with different resolutions over the sub-regions of interest. One application of this property is to refine the structural intensity near sources/sinks, where sharp changes exist in the velocity field.

For finite structures, the velocity on the boundaries of the measurement surface is not necessarily zero. As mentioned earlier, the resulting non-periodicity may cause great distortion in the wavenumber domain if SFT is directly performed. In order to minimise the distortion, windowing or mirror processing is often adopted. Since B-spline approximation does not assume that velocity is periodic at the boundaries, no special care is needed to treat the boundary conditions in this method. Fig. 3 shows an original velocity data compared to the data obtained by reconstructing the same data polluted with 15% white noise. The data along the four edges are not zero. That is, the non-periodic boundaries exist. It can be seen from Fig. 3(c) that the data can be reconstructed accurately through B-spline approximation, without any other special measures to deal with the non-periodic boundaries.

## 5. Experimental example

This section shows an example of calculating structural intensity through B-spline approximation. A simply supported plate excited by two phased shakers to act as energy source and sink is employed as the test object. The mesh size of the B-spline approximation is determined according to the relationship established in Eq. (10). The aim here is to examine whether the structural intensity calculated is able to locate the energy source/sink and determine the dominant path of power flow within the test plate.

Fig. 4 shows the diagram of the experimental set-up. The experiment was carried out on a 320 mm long and 230 mm wide aluminium plate, with a thickness of 2 mm. In order to

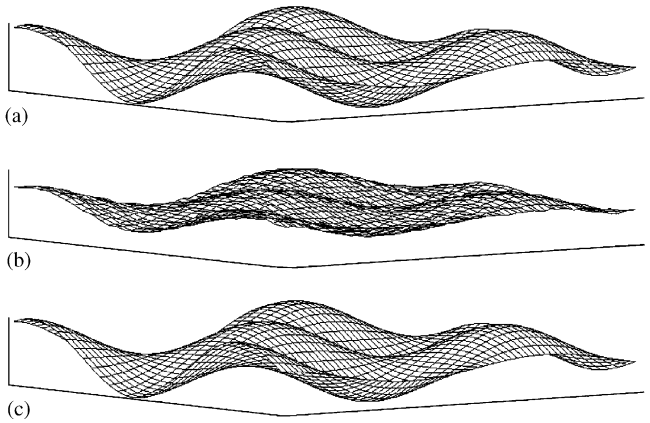


Fig. 3. Example of B-spline approximation: (a) original data; (b) data with 15% added noise; (c) data reconstructed with B-spline approximation.

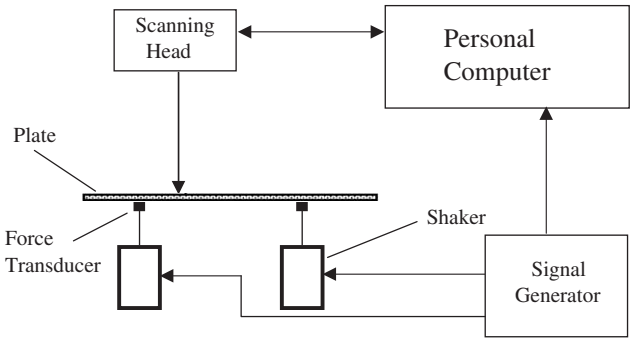


Fig. 4. Diagram of the experimental set-up.

demonstrate the capability of B-spline approximation to deal with non-periodic boundaries, the plate is mounted in such a way that two long edges are fixed to a rigid fixture with 6 screws and the other two short edges are set free. Two phased micro-shakers are employed to harmonically excite the plate with a constant frequency of 168 Hz. One arbitrary waveform generator and two force transducers are used to produce the two phased harmonic excitation signals and a PSV-300 scanning LDV is adopted to measure the vibration velocity. The schematic of the plate, the locations of the two shakers and the scanned area are shown in Fig. 5.

A complex velocity field over a $72 \times 50$ grid is scanned. Fig. 6 shows the root-mean-square (rms) velocity distribution. As expected, the velocities along all the four edges are not all zero due to the mounting conditions.

When excited harmonically at frequency $f$, the strong wavenumber components in the plate, correspond to the structural wavenumber defined by

$$k_s = \frac{\sqrt{2\pi f}}{\sqrt[4]{B/\rho}} \tag{11}$$

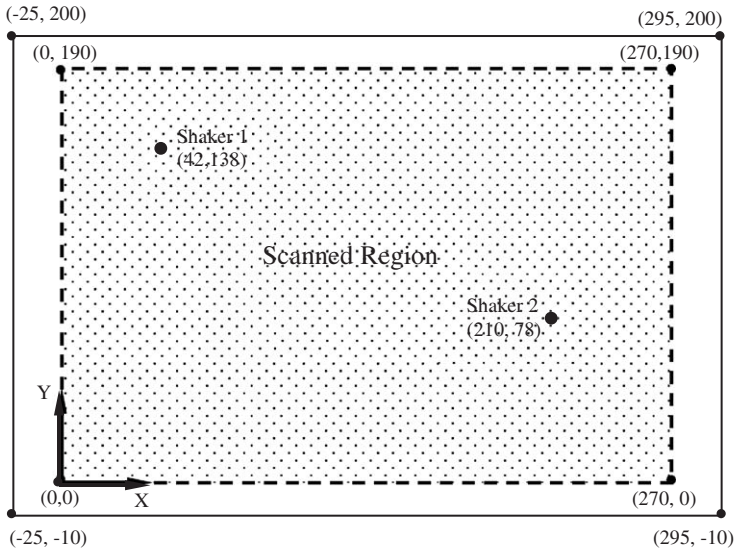


Fig. 5. Schematic of the test plate, scanned area and locations of the two shakers (dimension: mm).

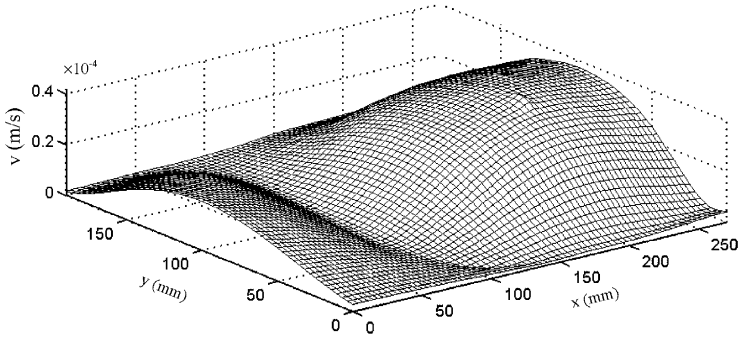


Fig. 6. Root mean square velocity distribution of the test plate with two shakers harmonically excited at 168 Hz.

and adjacent modes. $\rho$ is the mass per unit area. In order to reconstruct the measured velocity field, the scanned area is subdivided into $3 \times 2$ subrectangles uniformly. According to Eq. (10), the cut-off wavenumbers in $k_x$ and $k_y$ direction are 31.4 and 29.8, respectively, which are about 1.8 times as large as the structural wavenumber $k_s = 17.4$ estimated by Eq. (11). Therefore, the dominant wavenumber components are kept in the reconstructed velocity field, while noise at higher wavenumber is removed.

Fig. 7 shows the extracted structural intensity field over the plate using B-spline approximation. The two large black dots on the plot represent the relative size and location of the two shakers. It can be seen from Fig. 7 that the two shakers are clearly localised from the structural intensity map. Moreover, the intensity vectors around shaker 1 are convergent while those around shaker 2 are divergent. It implies that shaker 2 works as the energy source, however, shaker 2 works as an

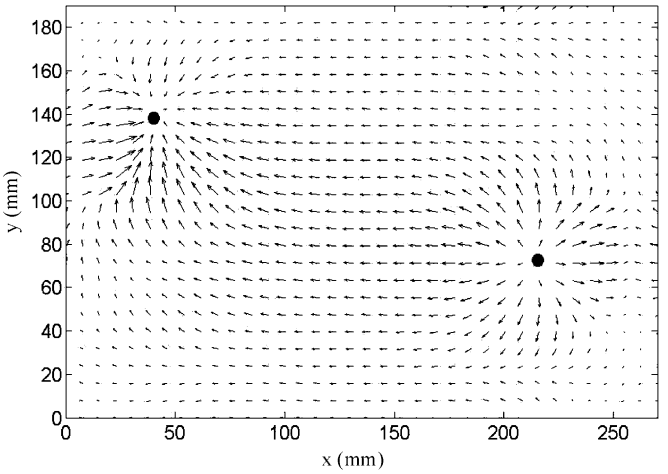


Fig. 7. Structural intensity vectors, calculated with B-spline approximation; two black dots indicate the locations of the shakers.

energy sink rather than a source during the excitation, and vibratory energy transmission does exist between the two shakers, similar to the results observed in Refs. [5,12].

In practice, structural intensity is usually used to locate the sources/sinks of energy and determine the dominant energy transmission path within the structure. If this is the case, it is clear that the mesh size chosen here fulfils the task successfully. When the accurate power injected into the structure is expected, a convergence procedure [12] may be employed to further determine the optimal mesh. However, with the knowledge of the relationship between mesh size and the $k$-space filtering, one can at least reduce the trial time to locate the proper mesh.

Some intensity vectors at the boundaries of Fig. 7 point to the wrong direction unexpectedly. It is not suggested that these are the correct values or representation of the structural intensity. One reason for this error is that less data is used to solve for the B-spline coefficients at the boundaries. Hence, it is suggested that a larger area than that of interest be scanned at the stage of velocity measurement.

## 6. Conclusion

The $k$-space filtering effect associated with the application of B-spline approximation in experimental determination of structural intensity is investigated. It is demonstrated that the B-spline approximation acts as a low-pass filter in the calculation, similar to the one usually used in SFT. The relationship between the mesh of the B-spline approximation and the $k$-space filtering is established. As B-spline approximation does not require the velocity data to be periodic in space and equally spaced, it has advantages over conventional method if the structure is geometrically complex. The structural intensity on a thin aluminium plate is calculated using B-spline approximation. The source/sink location and power flow distribution are clearly indicated without any special measures taken to deal with the arbitrary boundary conditions.

## References

[1] L. Gavric, G. Pavic, A finite element method for computation of structural intensity by the normal mode approach, *Journal of Sound and Vibration* 164 (1) (1993) 29–43.
[2] D.U. Noiseux, Measurement of power flow in uniform beams and plates, *Journal of the Acoustical Society of America* 47 (1970) 238–247.
[3] G. Pavic, Measurement of structure borne wave intensity—part I: formulation of the methods, *Journal of Sound and Vibration* 49 (2) (1976) 221–230.
[4] J.W. Verheij, Cross-spectral density methods for measuring structure borne power flow on beams and pipes, *Journal of Sound and Vibration* 70 (1) (1980) 133–138.
[5] E. Williams, H. Dardy, R. Fink, A technique for measurement of structure-borne intensity in plates, *Journal of the Acoustical Society of America* 78 (1985) 2061–2068.
[6] S.I. Hayek, M.J. Pechersky, B.C. Suen, Measurement and analysis of near and far field structural intensity by scanning laser vibrometery, in: *Proceedings of the Third International Congress on Intensity Techniques*, Senlis, France, 1990, pp. 281–288.
[7] R. Morikawa, K. Nakamura, S. Ueha, Structural intensity derivation using normal and in-plane vibration displacements measured by a laser Doppler vibrometer, in: *Proceedings of Inter-Noise*, Vol. 1, Newport Beach, USA, 1995, pp. 637–640.
[8] S.A. Hambric, Power flow and mechanical intensity calculations in structural finite element elements, *Journal of Vibration and Acoustics* 112 (1990) 542–549.
[9] R. Morikawa, S. Ueha, Error evaluation of the structural intensity measured with a scanning laser Doppler vibrometer and a *k*-space signal processing, *Journal of the Acoustical Society of America* 97 (1996) 2913–2921.
[10] J.C. Pascal, J.F. Li, X. Carniel, Wavenumber processing techniques to determine structural intensity and its divergence from optical measurements without leakage effects, *Shock and Vibration* 9 (2002) 57–66.
[11] J. Roberto, R. Arruda, Surface smoothing and partial spatial derivatives computation using a regressive discrete Fourier series, *Mechanical Systems and Signal Processing* 6 (1) (1992) 41–50.
[12] J.D. Blotter, R.L. West, S.D. Sommerfeldt, Spatially continuous power flow using a scanning laser Doppler vibrometer, *Journal of Vibration and Acoustics* 124 (2002) 476–482.
[13] L. Gavric, U. Carlsson, L. Feng, Measurement of structural intensity using a normal mode approach, *Journal of Sound and Vibration* 206 (1) (1997) 87–101.
[14] Y. Zhang, J.A. Mann III, Measuring the structural intensity and force distribution in plates, *Journal of the Acoustical Society of America* 99 (1996) 345–353.
[15] P. Dierckx, *Curve and Surface Fitting with Splines*, Oxford Science Publications, Oxford, 1993.
[16] A. Aldroubi, M. Unser, M. Eden, Cardinal spline filters: stability and convergence to the ideal interpolator, *Signal Processing* 28 (1992) 127–138.
[17] M. Unser, A. Aldroubi, M. Eden, B-spline signal processing, *IEEE Transactions on Signal Processing* 41 (1993) 821–833.